SAND2019-14525C

The effects of uncertain stochastic variations in Earth velocity structure on the inversion of seismic data for the time-domain moment tensor

Christian Poppeliers and Leiph Preston; Sandia National Laboratories, Albuquerque, NM

SAND2019-XXXXX

Introduction

Inversions of seismic data for an effective seismic source model is routinely performed as a discriminant between underground explosions and earthquake sources. Although linear inverse theory provides the mathematical machinery to propagate **DATA** uncertainty it is often **MODEL** uncertainty that is the greatest source of errors/uncertainty in seismic moment tensor inversions. We present a series of numerical simulations and inversions that evaluate the effects of model uncertainty on the estimates of the time-domain seismic moment tensor (TDMT), assuming noise-free data. The model uncertainty takes the form of high-wavenumber heterogeneities that would not be resolvable in, for example, tomographic inversions for seismic velocity. We build a smooth canonical model which we then perturb using a binary von Karman stochastic distribution of density and velocity. We find that the primary effects to synthetic data are its phase: the variance in the phase increases as time increases. However, there is no significant variation in the actual arrival time of the first-arriving seismic energy. Using a Monte Carlo method to invert for the TDMT, we find that the estimated amplitudes of the on-diagonal TDMT terms are higher than the actual amplitudes of the source model. Conversely, observe that the amplitude of the off-diagonal terms is approximately preserved, however, they contain more energy in the high frequency portions. Based on these tests, we conclude that inverting for the TDMT using a model with stochastic heterogeneities results in the energy in the isotropic source terms being "pushed" to the higher frequency components of the off-diagonal moment tensor terms.

Experiment Design

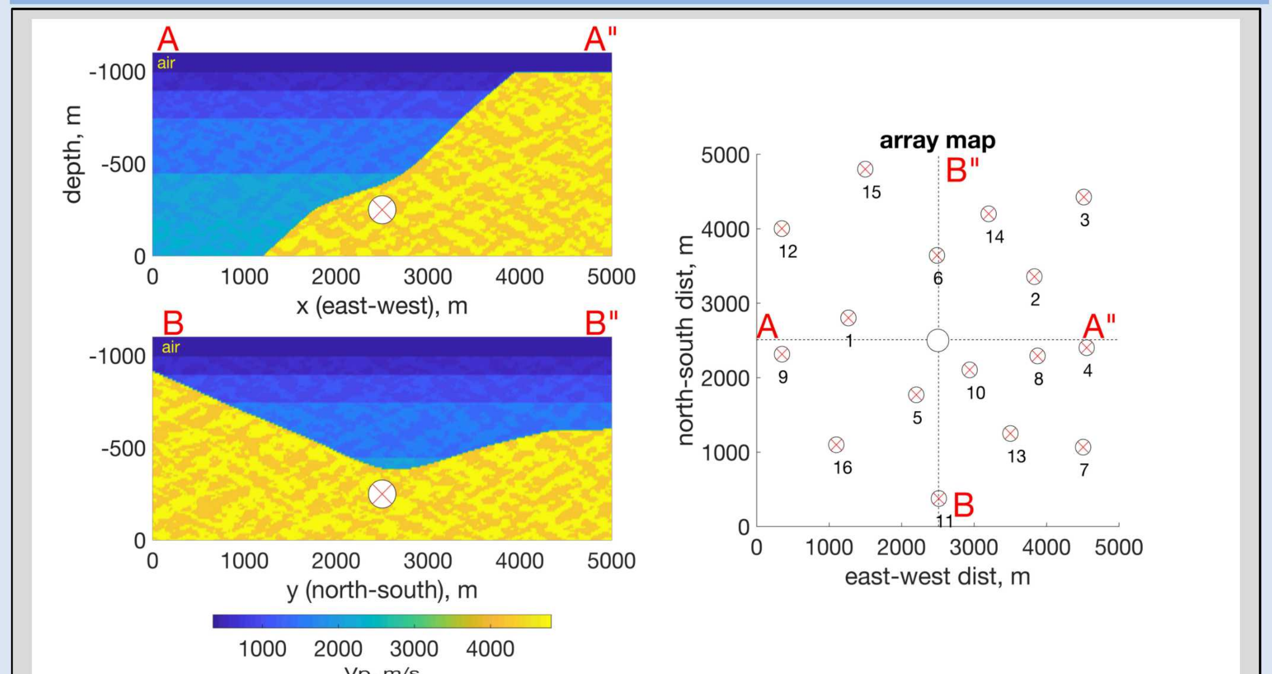

Figure 1: A single realization of an Earth model used for the simulations. The model consists of two major regions: a layered, sedimentary region juxtaposed next to an igneous region. Both regions contain bi-model stochastic heterogeneities with horizontal characteristic lengths of 600m, and a vertical characteristic length of 150m. The simulated data are collected on an array of 16 3-component stations.

Forward Model

We assume that seismograms at $\boldsymbol{x}'$ are a convolution of the Earth's impulse response with a series of time-varying body forces:

$$u_k(\boldsymbol{x}',t') = \sum_{i=1}^{N_s} \int_{-\infty}^{\infty} G^{(i)}(\boldsymbol{x}',t';\boldsymbol{x},t)S^{(i)}(\boldsymbol{x},t)dt, \quad (1)$$

where $\boldsymbol{G}^{(i)}$ is the source-to-receiver elastic Green's function for the i^{th} component of the moment tensor and $\boldsymbol{S}^{(i)}$ is the source time function of the i^{th} Green's function component. To simulate the seismograms, we model the explosion source as under-buried, and hence, non-isotropic: $M_{xx}(t)=M_{yy}(t)=0.6M_{zz}(t)$. We model the (co-located) earthquake source as a double couple source with a strike, dip, and rake of 10, 60, and 45 degrees, respectively. The total energy of the earthquake source is half that of the explosion source. Note that the source time function of the explosion is different than that of the earthquake.

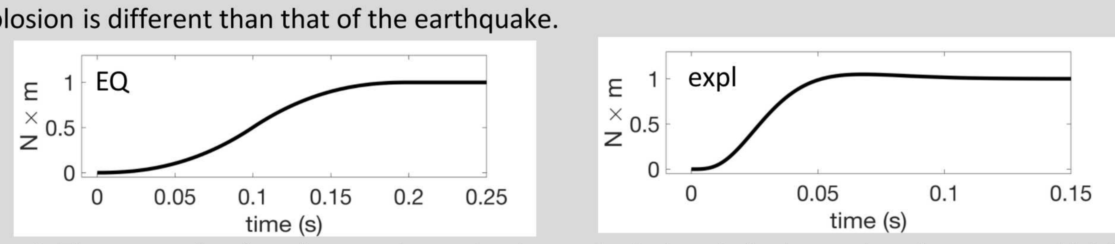

Figure 2: The source time functions used to make the synthetic data. Left: the earthquake source, which is scaled by the off-diagonal moment tensor components (M_{xy}, M_{xz}, M_{yz}). Right: the explosion source, which is scaled by the on-diagonal moment tensor components (M_{xx}, M_{yy}, M_{zz}).

Inverse Method

Equation (1) is recast in the frequency domain

$$u(f) = \sum_{i=1}^{6} G^{(i)}(f)S^{(i)}(f) \quad (2)$$

where $\boldsymbol{S}^{(i)}$ are the spectra of the source terms. In matrix form, equation 2 is written as

$$\boldsymbol{u} = \boldsymbol{GS} \quad (3)$$

and solved for $\boldsymbol{S}$ using generalized least squares. The term $\boldsymbol{S}$ contains the complex spectra of the estimated source terms.

Monte Carlo Experiments

Experimental Philosophy: Although we can obtain high-quality estimates of the large-scale deterministic velocity structure, we cannot capture the high-wavenumber heterogeneities. The high-wavenumber heterogeneities are responsible for scattering, especially at higher frequencies, and are the largest source of uncertainty in our model.

Experimental Goals: 1) How do the uncertainties and magnitude of the high-wavenumber stochastic heterogeneities propagate into the data?
2) How do these uncertainties impact our estimation of the seismic source?

Experimental Procedure: Construct synthetic velocity models with realistic geologic structure and superpose stochastic heterogeneities. Perform Monte Carlo tests to understand the effects, in a statistical sense, that the high-wavenumber uncertainties has on the data as well as the inversion of the data for the seismic source attributes.

Experiment 1: How does stochastic heterogeneity effect data?

Experiment 1: Generate a single stochastic realization of the heterogeneities and apply it to a deterministic Earth velocity model. We used a bimodal von Karman distribution to generate the stochastic heterogeneities, where the magnitude of the velocity heterogeneities are 2.5%, 5.0%, and 7.0%, and the characteristic lengths of the 3D stochastic field is $a_x=a_y=600$m, $a_z=150$m.

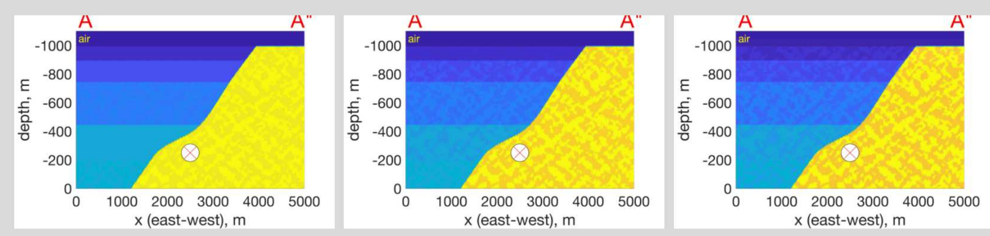

Figure 3: The P-wave velocity models used to generate the synthetic data for the tests shown here. For each model shown we varied the magnitude of the velocity heterogeneity to be ±2.5% (left), ±5.0% (middle), and ±7.5% (right) of the local background velocity. The shear wave velocity was determined by the relationship Vs = 0.7Vp.

1) Generate synthetic data for each model using a 3D finite difference approximation to the elastic wave equation.

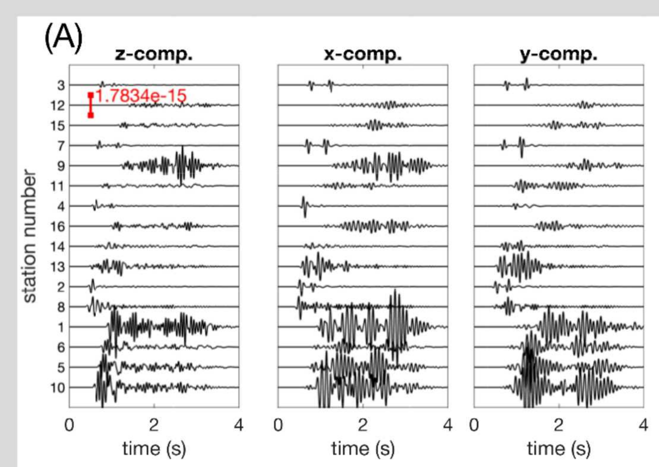

Figure 4: The synthetic data, where the velocity heterogeneities varied by 7.5%. All of the seismograms are normalized to station 10, and are arranged in order of increasing distance from the source epicenter. The red text indicates the amplitude, in m/sec.

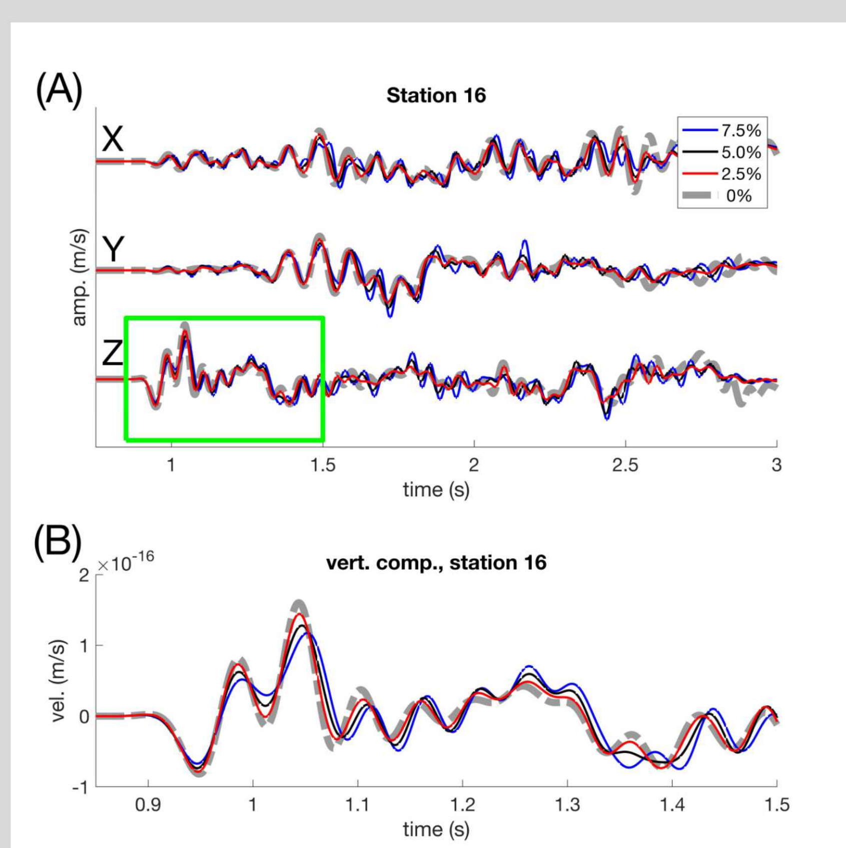

Figure 5: An example of the effects of stochastic heterogeneities. Panel A shows a three component seismogram for a single station, for the baseline model (i.e. no stochastic heterogeneities) in gray, as well as the seismograms for the models that contain stochastic velocity perturbations of 2.5% (red), 5.0% (black), and 7.5% (blue). Panel B shows an enlarged view of the z-component seismogram (indicated by the green box in Panel A). Note that as the degree of heterogeneities' velocity perturbation increases, the amplitude of the first arriving seismic energy decreases. This energy is scattered into later portions of the seismogram.

Experiment 2: To evaluate how model uncertainty propagates into the data in a probabilistic sense, we performed Monte Carlo simulations. We constructed a suite of models, each with a different stochastic realization, and for each stochastic realization, generate synthetic data.

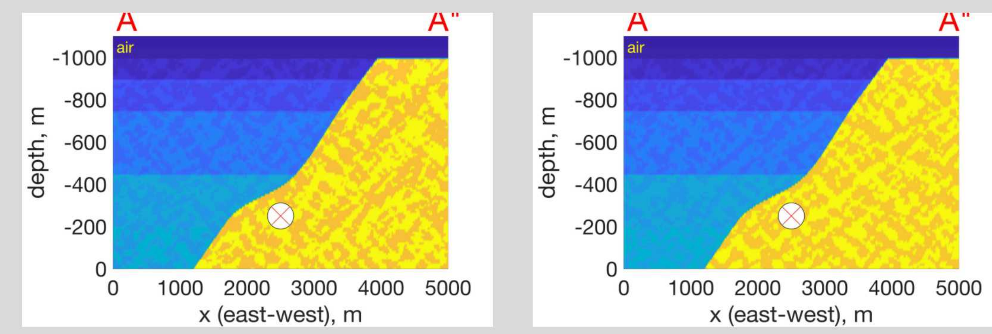

Figure 6: Two stochastic realizations of the P-wave velocity model. For each model, the deterministic structure is identical, as are the characteristic lengths of the stochastic heterogeneities. However, for each model, the random phase is different, leading to a different realization of the stochastic field.

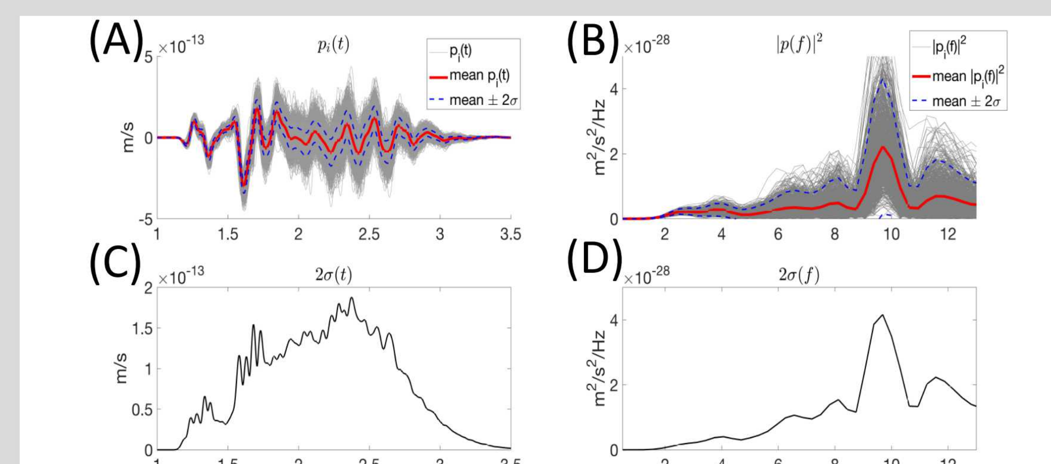

Figure 7: The y-component seismogram of station 15, computed using 1000 stochastic realizations of the velocity model used here. In Panel A, the thin gray lines are the individual seismograms, with the mean (red) and two standard deviations 2σ about the mean (blue dashed). The key observation is that for this type of model uncertainty, the arrival time of is not effected. Rather, the phase of individual arrivals are effected. Note that the phase variance increases with increasing time, which is the result of scattering by the heterogeneities. This is shown in Panel C, where the width of the 2σ increases through time until the amplitude of the seismogram decreases. In Panels B and D, we see similar behavior in the power spectrum: the variance in the power spectrum generally increases as frequency increases.

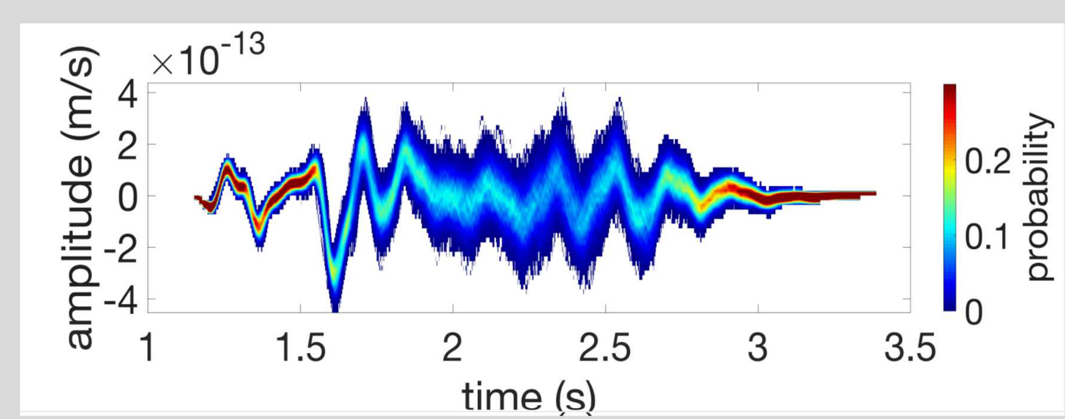

Figure 8: The same seismogram as shown in Figure 7, Panel A, except shown as a probability density function (PDF). This representation highlights the primary effects of this type of model uncertainty: Specifically, the first-arriving energy (in this case, t<1.5 seconds) is not as effected by the uncertainty as the later portions of the seismogram. The PDF for t<1.5 seconds is "tall and narrow", whereas the PDF for later portions of the seismogram become "shorter and wider" as time increases.

Interpretation and Implications:

1) The earlier (in time) portions of the seismogram are less effected by model uncertainty.
2) Lower frequency portions of the seismograms are less effected by model uncertainty
3) This implies that when inverting seismograms for the moment tensor that
   - The earlier portions of the estimated moment tensor terms will have less uncertainty than the later portions
   - The estimated moment tensor components will be less certain at higher frequencies

Experiment 2: How does stochastic heterogeneity effect inversion?

Experimental Procedure: Generate synthetic data using a single realization of the stochastic velocity model. Invert this data, *N* times where each inversion uses a different stochastic realization of the velocity model. Compile the results and compute the PDFs.

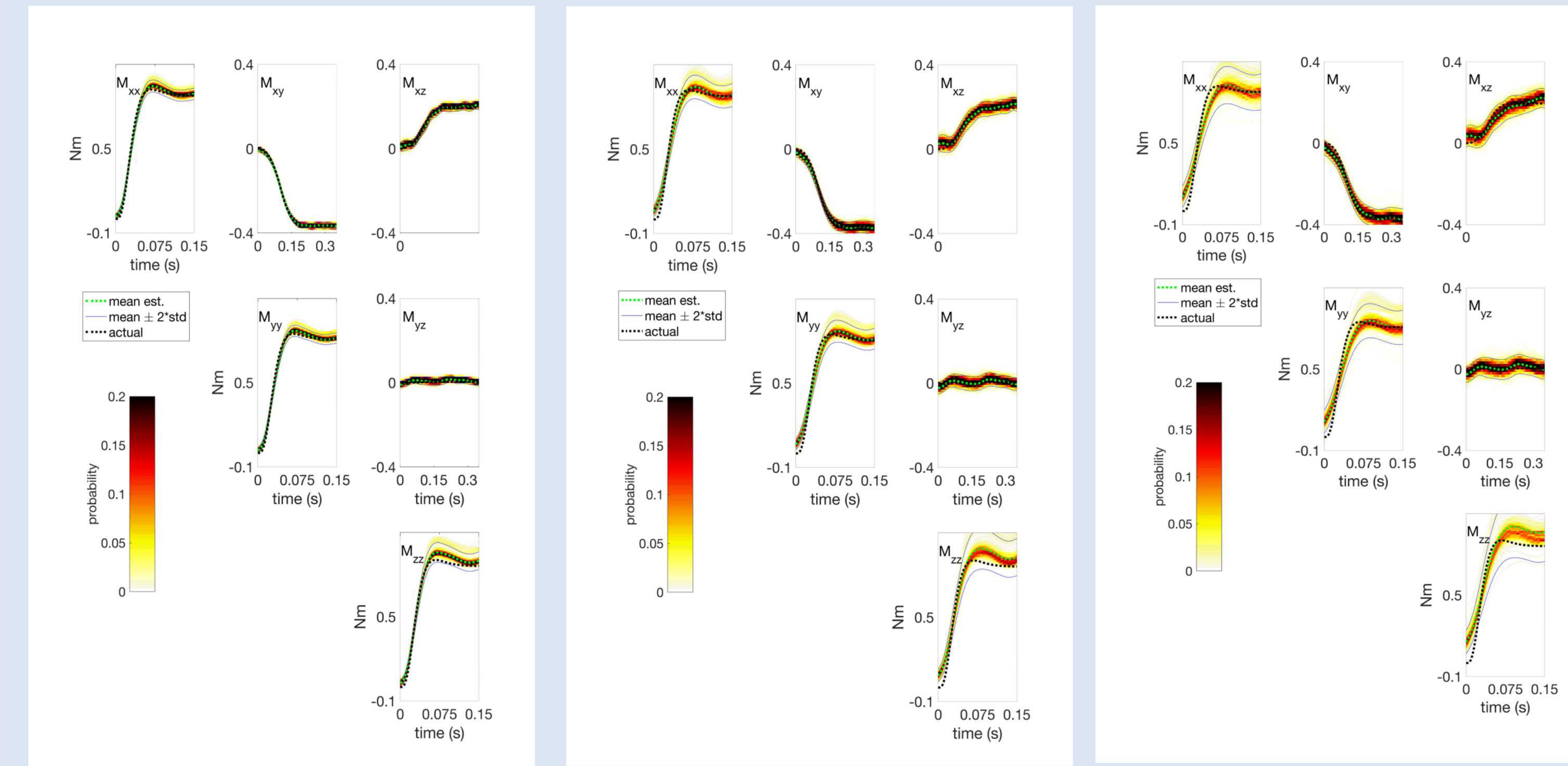

Figure 9: Results of inverting the data shown in Figure 4. The figure shows the six independent time domain moment tensor components for 300 Monte Carlo simulations, where the magnitude of the stochastic variation was ±2.5% (A), ±5.0% (B), and ±7.5% (C) of the local background velocity. For each Monte Carlo simulation, the data were inverted using Green's functions estimated for a different realization of the stochastic model shown in Figure 3. The results of each inversion are compiled and then presented as a PDF. As the magnitude of the stochastic velocity perturbation increases, the variance (as indicated by the standard deviation σ about the mean estimated moment tensor) increases as well. The degree of uncertainty, as measured by the width of the PDF at a given time, is correlated with the magnitude of the stochastic velocity perturbations. Note also that the model uncertainty causes the mean of the on-diagonal moment tensor terms (e.g. the explosion portion of the model) to overshoot the actual value of the moment tensor. However, the mean of the off-diagonal moment tensor estimates (the double-couple earthquake components) are quite close to the actual values.

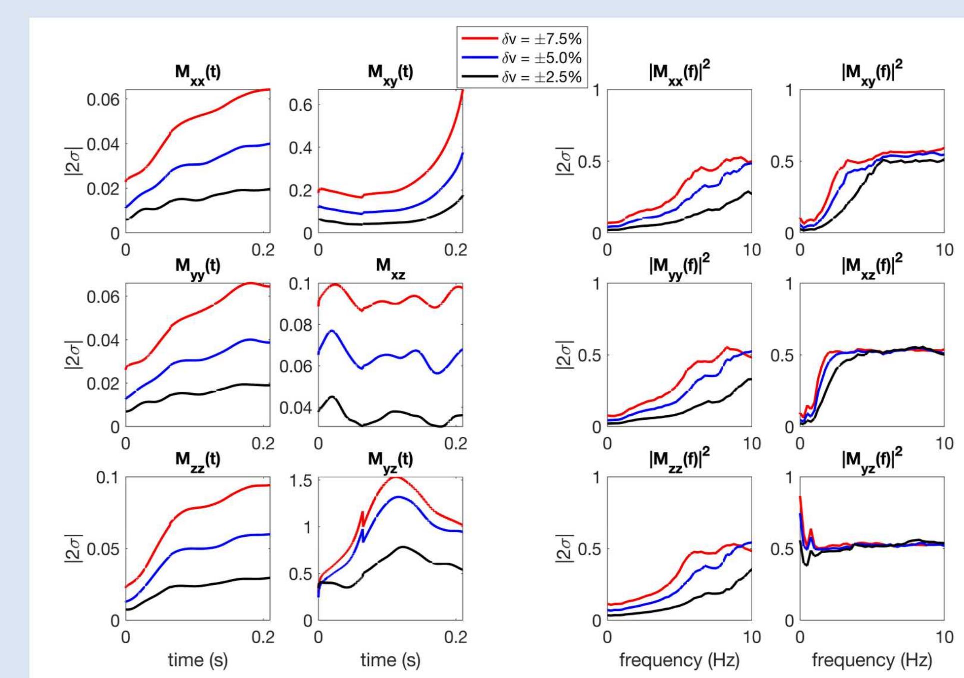

Figure 10: The magnitude of 2σ, as a function of time (A) and frequency (B) for the estimated moment tensors (shown in Figure 9). As magnitude of 2σ increases, the uncertainty in the estimated moment tensor component increases. Note that 2σ generally increases with time and frequency. Also note that increasing the percent velocity perturbation increases the uncertainty in the estimates of the moment tensor components.

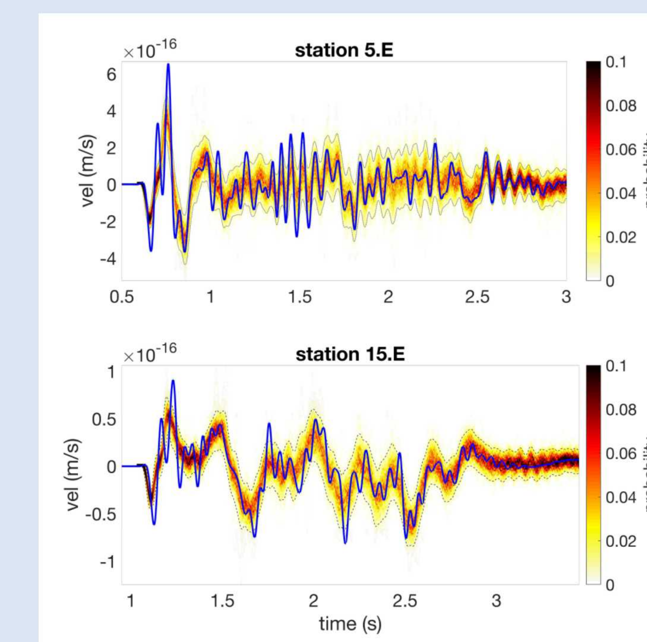

Figure 11: The fit to data, for stations 5 and 15 (for the 7.5% velocity perturbation), shown as a PDF. To make this figure, we used the N estimates of the moment tensor terms to solve $\boldsymbol{d}_{\mathbf{pred}} = \boldsymbol{Gm}$, (equation 3) where $\boldsymbol{G}$ are the *N* estimated Green's functions from the *N* stochastic models used to invert the data. Note how the uncertainty is quite low at the first arrival, and increases through time. Also, note how the actual data appears to have a higher frequency content than the mean of the PDF.

Take-away points

1. Model uncertainty is the largest source of error in seismic moment tensor inversions.
2. We simulate model uncertainty using a stochastic, bimodal velocity perturbation, which is described by a von Karman distribution.
3. The model uncertainty does not effect the timing of the first-arriving seismic energy. Rather, it effects the phase of the data. This phase distortion increases through time. This means that the model Green's functions become more uncertain for increasing time.
4. Because the uncertainty of the Green's functions increase with time, the uncertainty in the estimated moment tensor components increase through time.
5. The uncertainty in the in the estimated Green's functions appears to cause the predicted data to have a lower frequency content than the actual data.

Acknowledgments

We acknowledge the National Nuclear Security Administration Defense Nuclear Nonproliferation Research and Development (DNN R&D)

Sandia National Laboratories is a multimission laboratory managed and operated by National Technology and Engineering Solutions of Sandia LLC, a wholly owned subsidiary of Honeywell International Inc. for the U.S. Department of Energy's National Nuclear Security Administration under contract DE-NA0003525.